



Long-term oral kinetin does not protect against α -synuclein-induced neurodegeneration in rodent models of Parkinson's disease



Adam L. Orr ^a, Florentine U. Rutaganira ^b, Daniel de Roulet ^c, Eric J. Huang ^d,
Nicholas T. Hertz ^c, Kevan M. Shokat ^{b,c}, Ken Nakamura ^{a,e,*}

^a Gladstone Institute of Neurological Disease, Gladstone Institutes, San Francisco, CA, USA

^b Howard Hughes Medical Institute and Department of Cellular and Molecular Pharmacology, University of California, San Francisco, San Francisco, CA, USA

^c Mitokinin LLC, 2 Wall Street, 4th Floor, New York, NY, USA

^d Department of Pathology, University of California, San Francisco, San Francisco, CA, USA

^e Department of Neurology, University of California, San Francisco, San Francisco, CA, USA

ARTICLE INFO

Article history:

Received 29 January 2017

Received in revised form

20 March 2017

Accepted 11 April 2017

Available online 20 April 2017

Keywords:

PINK1

α -Synuclein

Kinetin

Neurodegeneration

Parkinson's disease

Adeno-associated virus

AAV

ABSTRACT

Mutations in the mitochondrial kinase PTEN-induced putative kinase 1 (PINK1) cause Parkinson's disease (PD), likely by disrupting PINK1's kinase activity. Although the mechanism(s) underlying how this loss of activity causes degeneration remains unclear, increasing PINK1 activity may therapeutically benefit some forms of PD. However, we must first learn whether restoring PINK1 function prevents degeneration in patients harboring PINK1 mutations, or whether boosting PINK1 function can offer protection in more common causes of PD. To test these hypotheses in preclinical rodent models of PD, we used kinetin triphosphate, a small-molecule that activates both wild-type and mutant forms of PINK1, which affects mitochondrial function and protects neural cells in culture. We chronically fed kinetin, the precursor of kinetin triphosphate, to PINK1-null rats in which PINK1 was reintroduced into their midbrain, and also to rodent models overexpressing α -synuclein. The highest tolerated dose of oral kinetin increased brain levels of kinetin for up to 6 months, without adversely affecting the survival of nigrostriatal dopamine neurons. However, there was no degeneration of midbrain dopamine neurons lacking PINK1, which precluded an assessment of neuroprotection and raised questions about the robustness of the PINK1 KO rat model of PD. In two rodent models of α -synuclein-induced toxicity, boosting PINK1 activity with oral kinetin provided no protective effects. Our results suggest that oral kinetin is unlikely to protect against α -synuclein toxicity, and thus fail to provide evidence that kinetin will protect in sporadic models of PD. Kinetin may protect in cases of PINK1 deficiency, but this possibility requires a more robust PINK1 KO model that can be validated by proof-of-principle genetic correction in adult animals.

© 2017 Elsevier Ltd. All rights reserved.

1. Introduction

Parkinson's disease (PD) is characterized by the progressive loss of dopaminergic (DA) neurons in the substantia nigra (SN). Mitochondrial dysfunction likely plays a central role in this process, although its underlying mechanisms are poorly understood (Haddad and Nakamura, 2015). Mutations in PTEN-induced putative kinase 1 (PINK1) cause rare inherited forms of PD (Valente et al., 2004; Ricciardi et al., 2014), providing the first direct genetic evidence that mitochondrial dysfunction can cause PD.

Heterozygous mutations in PINK1 are also a risk factor for sporadic PD (Puschmann et al., 2017). Most, if not all, PD-causing mutations in PINK1 disrupt PINK1's kinase function (Song et al., 2013), implicating that loss of PINK1 kinase activity causes PD. However, the mechanism by which PINK1 kinase activity supports DA neuron function and survival remains unknown. Additionally, PINK1 can accumulate on mitochondria, which facilitates the degradation of damaged mitochondria through a Parkin-dependent mechanism (Narendra et al., 2008, 2010). This process depends on PINK1's direct phosphorylation of ubiquitin and Parkin (Kane et al., 2014; Koyano et al., 2014). PINK1 kinase activity also regulates both complex I function and mitochondrial transport in axons via phosphorylation of NDUFA10 (Morais et al., 2014) and the adaptor protein Miro, respectively (Wang et al., 2011). PINK1 may also

* Corresponding author. Gladstone Institute of Neurological Disease, Gladstone Institutes, 1650 Owens Street, San Francisco, CA 94158, USA.

E-mail address: ken.nakamura@gladstone.ucsf.edu (K. Nakamura).

regulate mitochondrial dynamics (Poole et al., 2008; Itoh et al., 2013). Furthermore, PINK1 exerts mitochondria-independent effects (Lin et al., 2014; Haque et al., 2008; Dagda et al., 2014), and the relative contributions of these non-mitochondrial pathways to degeneration in PD remain unknown.

Due to the complex, yet incompletely defined, roles of PINK1 in maintaining neuronal viability, we do not know if targeting a single PINK1 function can prevent degeneration and, if so, which function. However, given the importance of PINK1 kinase activity in mediating PINK1 functions, directly augmenting its activity is a particularly promising therapeutic approach. Recently, we identified an ATP analog, kinetin triphosphate (KTP), that increases the maximal catalytic activity of both wild-type (WT) and a mutant form of PINK1 (G309D) (Hertz et al., 2013), raising the possibility that this ATP analog might be used to pharmacologically boost or restore PINK1 activity in both sporadic and inherited forms of PD. Kinetin, the biologically available precursor to KTP, protects neural cells against oxidative stress *in vitro* and influences mitochondrial transport in primary neurons. Kinetin has been safely administered to rodents and humans, and it can accumulate in brain tissue (Shetty et al., 2011; Gold-von Simson et al., 2009); however, it has not been tested for its capacity to prevent neurodegeneration.

To establish PINK1 activation as a promising therapeutic approach for PD, we must first validate the approach in a model of PINK1-based DA-neuron degeneration. However, while PINK1 knockout (KO) or mutant flies have systemic phenotypes, including severe muscle degeneration associated with severe mitochondrial dysfunction (Clark et al., 2006; Park et al., 2006), PINK1 KO mice show only altered dopamine homeostasis without neurodegeneration (Kitada et al., 2007). In contrast, loss of PINK1 in rats causes many behavioral phenotypes between 2 and 8 months of age, prominent changes in catecholamine levels by 8 months of age and, most importantly, loss of ~50% DA neurons in the SN by 8–9 months of age (Dave et al., 2014; Villeneuve et al., 2016). However, this degeneration was not observed in a study that used a non-stereological method of quantitation (Grant et al., 2015).

As homozygous or compound heterozygous PINK1 mutations are an extremely rare cause of recessive PD, while heterozygous mutations are a risk factor for sporadic PD (Puschmann et al., 2017), it would also be important to determine whether a PINK1-based therapy protects in sporadic PD. However, sporadic PD is likely heterogeneous, and there is no accepted animal model for it. Among the existing models, rodents overexpressing α -synuclein may be most representative. Indeed, sporadic PD is characterized by the accumulation of α -synuclein in neuronal processes and at the cell body (Spillantini et al., 1998), while a subset of familial PD is caused by mutations in α -synuclein or increased expression of WT α -synuclein (Polymeropoulos et al., 1997; Kruger et al., 1998; Zarranz et al., 2004; Singleton et al., 2003; Ibanez et al., 2004). Boosting PINK1 function may protect against α -synuclein toxicity in PD. For example, α -synuclein interacts with mitochondria in midbrain neurons (Devi et al., 2008; Nakamura et al., 2011; Li et al., 2007), and increased levels of α -synuclein reduce mitochondrial complex I levels and activity (Devi et al., 2008; Loeb et al., 2010; Liu et al., 2009; Chinta et al., 2010), similar to the effects of PINK1 deficiency (Morais et al., 2009, 2014).

Additionally, DA neurons are susceptible to the neurotoxin 1-methyl-4-phenyl-1,2,3,6-tetrahydropyridine (MPTP), an effect ameliorated by α -synuclein KO (Dauer et al., 2002) and potentiated by PINK1 KO (Haque et al., 2012). Further, overexpression of α -synuclein causes mitochondrial fragmentation (Nakamura et al., 2011) that can be rescued by PINK1 (Kamp et al., 2010), and the toxicity of mutant A53T α -synuclein is exacerbated when PINK1 is absent (Gispert et al., 2015). Therefore, these two PD-related genes appear to interact, at least indirectly, through their common effects

on mitochondrial function.

Augmenting PINK1 kinase activity could benefit both sporadic and inherited forms of PD. Thus, we hypothesized that pharmacologically activating PINK1 might prevent the selective degeneration of DA neurons in PINK1 KO rats and the pathologic and behavioral deficits in two rodent models of α -synuclein-induced PD.

2. Materials and methods

2.1. Animals

All experimental animals were males, because prior studies reporting neurodegeneration in PINK1 KO rats were performed exclusively in males (Dave et al., 2014; Grant et al., 2015) or were not reported (Villeneuve et al., 2016). Colonies of WT and PINK1 KO Long-Evans Hooded rats were established from founders obtained from SAGE Labs. PCR genotyping of tail DNA was performed as described (Dave et al., 2014). Quantitative real-time PCR analysis of PINK1 expression in brain tissue from WT and PINK1 KO rats was determined using the Taq-Man Cells-to-CT kit (Life Technologies) with PINK1 expression normalized to mouse 18S rRNA. Ten-week-old male Sprague-Dawley rats were from Charles River. Mice overexpressing human WT α -synuclein under the Thy1 promoter (Thy1-hSyn line 61) have been described (Rockenstein et al., 2002). Additional 10-week-old male C57BL/6J mice were obtained from The Jackson Laboratory for pilot trials with the kinetin chow. Rodent colonies were maintained with a standard 12 h light/dark cycle and given food and water *ad libitum*. Body weights and chow intake were monitored at least twice weekly, and food and hydration gels were placed on the floor of cages of any animals displaying weight loss or signs of distress. Animals were euthanized if body weights decreased by more than 15% of peak weight. Experiments were conducted in accordance with the Guide for the Care and Use of Laboratory Animals, as adopted by the National Institutes of Health, and with approval of the University of California, San Francisco Institutional Animal Care and Use Committee.

2.2. Kinetin chow

Kinetin (ChemImpex International) was delivered orally to both mice and rats in their chow following published reports (Shetty et al., 2011). Rodent chow (Purina 5 053) was formulated by Research Diets (New Brunswick, NJ) to contain 5.25 g kinetin with 25 g Smokey Bacon Flavoring (Gold Coast Ingredients, Commerce, CA) or 3.50 g kinetin alone per kg chow for rats or mice, respectively. Based on weight gain and levels of chow consumption relative to controls, these amounts of kinetin were well tolerated by each species during prolonged dose escalation trials. These levels of kinetin correspond to an average of 400 or 300 mg kinetin/kg body weight/day for mice or rats, respectively. Chow was stored at -20°C or below until the morning of feeding and fresh chow was provided at least every four days. Due to incorporation of differently colored food dyes in each chow formulation, the delivery of chow was not blinded with respect to drug treatment. Drug delivery to Thy1-hSyn mice, but not PINK1 KO rats, was blind to genotype as the PINK1 KO rats were visibly heavier than WT rats.

2.3. Adeno-associated viruses

WT and G309D mutant PINK1 were PCR amplified from vectors described previously (Hertz et al., Cell, 2013) with the C-terminal addition of V5 epitopes and AgeI (5') and NotI (3') sites. Gel purified PINK1-V5 DNA was subcloned into the pTR-CBA-eGFP vector (a gift from Dr. R. Jude Samulski, University of North Carolina) to replace eGFP. SURE 2 Supercompetent Cells (Agilent Technologies) were

transformed with pTR-CBA-PINK1-V5 constructs, and inverted terminal repeat (ITR) integrity was verified by sequencing and XmaI digestion prior to production of adeno-associated virus (AAV)2/6 particles by the University of North Carolina Vector Core. Titers were 6.2×10^{12} and 4.5×10^{12} viral genomes/ml for PINK1-WT-V5 and PINK1-G309D-V5, respectively. Expression of full-length PINK1-V5 was verified in primary hippocampal neurons by Western blotting. Expression in midbrain DA neurons *in vivo* was demonstrated by confocal microscopy prior to their reintroduction into PINK1 KO rats.

AAV2/2-CBA-human- α -synuclein particles (hereafter referred to as AAV- α -synuclein or Syn; 1.5×10^{13} viral genomes/ml) were provided by the Michael J. Fox Foundation via the University of North Carolina Vector Core.

2.4. Culture and immunostaining of primary neurons

Postnatal hippocampal neurons were cultured from P0 rat pups as described (Pathak et al., 2015). Expression of PINK1-V5 and its localization to mitochondria were tested by infecting neurons at DIV4 with AAV-PINK1-V5 (WT or G309D). At DIV7, neurons were treated overnight with 10 μ M carbonyl cyanide-4-(trifluoromethoxy)phenylhydrazone (FCCP; Sigma), fixed with 4% paraformaldehyde in phosphate-buffered saline (PBS), and immunostained and imaged for the mitochondrial marker Tom20 (rabbit, Santa Cruz Biotechnology, SC-11415, 1:1000) and the V5 epitope (mouse, Life Technologies, R960-25, 1:1000) as described (Pathak et al., 2015). Expression of full-length PINK1-WT/G309D-V5 in cell lysates was determined by infecting neurons at DIV5 with PINK1-WT-V5 or PINK1-G309D-V5 viruses. At DIV9, neurons were treated overnight with 10 μ M FCCP (Sigma), harvested in SDS-PAGE loading buffer, and immunoblotted as described (Orr et al., 2015) for PINK1 (rabbit, Novus Biologicals, BC100–494, 1:500) and actin (mouse, EMD Millipore, MAB1501R, 1:1000).

2.5. Stereotaxic injection of AAV

Intracranial injections of AAV into the ventral midbrain were performed on 10-week-old rats. Rats were anesthetized with a mixture of ketamine (Ketaset; Butler Schein, 100 mg/kg) and xylazine (Anased, Butler Schein, 10 mg/kg) and secured in a stereotaxic frame (Kopf). Animals were given buprenorphine (Buprenex, Butler Schein, 0.05 mg/kg) for analgesia just before and the morning after surgery. Viruses were injected undiluted (α -synuclein) or diluted 1:6 (PINK1-G309D-V5) or 1:8 (PINK1-WT-V5) in PBS just before injection. For all viruses, PBS was also used for control injections. Viruses were injected bilaterally at a rate of 0.4 μ L/min using a 10 μ L Hamilton syringe and a blunt-ended needle (32 gauge). Mixed bilateral injections of different viruses or PBS were made into the SN pars compacta (SNc; anteroposterior, -5.2 mm from bregma; mediolateral, ± 2 mm from midline; dorsoventral, -7.7 mm below skull) with each rat receiving a different virus or PBS injection into each hemisphere. A small pocket was created by inserting the needle to a depth of -7.8 mm below the skull, holding for 1 min, and then retracting to -7.7 mm just before injection. After injection, the needle was held in place for 5 min before retraction. Surgery and recovery occurred on heating pads. Animals were provided with hydration gel, wet chow, and assorted food treats on the floor of their cage for at least 24 h post-surgery and were monitored for signs of pain, dehydration, and weight loss. Rats were sacrificed 4 weeks after α -synuclein injection or 5.5 months after PINK1-WT/G309D-V5 injections. Proper targeting of viruses to the SNc was confirmed by immunofluorescent labeling (see section 2.8) and visual observation of needle tracts. All animals displayed proper targeting

although 5 rats injected on the same day with α -synuclein did not show any viral expression and were excluded from further analyses.

2.6. Brain kinetin and dopamine levels

All chemical analyses were performed with the examiner blind to genotype and drug group. For collection of tissue for biochemical analyses, animals were euthanized by CO₂ asphyxiation followed rapidly by cervical dislocation and dissection of brain tissue. Kinetin was extracted from cortical tissue that was flash frozen on dry ice and stored at -80 °C until analysis. Naive brain tissue and calibration standards of kinetin (Sigma-Aldrich K3378, Lot 103M4072V) were extracted in parallel to controls and for building a standard curve. Caffeine (Sigma-Aldrich C8960, Batch 068K0043) was included as an internal standard. Kinetin and caffeine calibration standards were dissolved in 0.1 M hydrochloric acid, and stock solutions were stored at 4 °C in glass vials wrapped in foil. Kinetin stock solutions were diluted with water to prepare calibration standard solutions between 5 and 10,000 pg/mg tissue and spiked into 100 mg samples of naive brain tissue (weighed out while frozen into microfuge tubes) to generate a standard curve. Naive samples were sequentially vortexed for 30 s in 50 μ L of ice-chilled water, 10 s after the addition of 10 μ L of 0.5 μ g/mL caffeine, 10 s after the addition of 10 μ L of kinetin calibration standards, and a final 10 s after the addition of 300 μ L of acetonitrile. For the extraction of kinetin from brains of treated animals, 10 μ L of water was used instead of kinetin calibration standard. Extracted samples were centrifuged for 20 min at 4 500 g at 4 °C, and supernatants were transferred to 2 mL vials and evaporated with a Genevac EZ evaporator. Samples were reconstituted by sonicating at room temperature for 10 min in 100 μ L of 0.1% formic acid in water. Samples were centrifuged for 3 400 g for 5 min at room temperature using EMD Millipore Ultrafree-MC 0.22 μ m Durapore PVDF filter tubes and transferred to QsertVials (Supelco). Samples (5 μ L) were injected onto an Acquity UPLC BEH C18 (1.7 μ m) column using 5% acetonitrile and 0.1% formic acid in water as the mobile phase with an acetonitrile gradient of 5–40% over 1.8 min at 600 μ L/min. The LC-MS/MS system consisted of a Waters Acquity UPLC coupled to a Waters Acquity TQD. Waters Intellistart was used to develop a MRM method for kinetin and caffeine infused at 500 μ M in 5% DMSO, 47.5% acetonitrile, 0.1% formic acid, and 47.5% water with argon as the collision gas. ESI-MS/MS analysis was performed in the positive mode with Intellistart-optimized conditions for kinetin (MRM precursor 216.07 > transition 80.96, cone voltage 16, collision energy 22; MRM precursor 216.07 > transition 53.01, cone voltage 16, collision energy 40) and caffeine (MRM precursor 194.1 > transition 116.90, cone voltage 8, collision energy 4). Kinetin content was normalized to the starting wet weight of brain tissue for each sample.

To measure striatal dopamine content, rat brains were placed in a rodent brain matrix (ASI International, Warren, MI) chilled on ice, and two coronal sections (2 mm thick) were removed beginning at the head of the striatum using clean, chilled razor blades. From each hemisphere, tissue punches were taken from the dorsal striatum using chilled wide-bore plastic pipette tips (Rainin, Mettler Toledo) and flash frozen in Eppendorf tubes on dry ice. Total dopamine content was measured by the Vanderbilt Neurochemistry core, as described previously (Berthet et al., 2014; Hnasko et al., 2010), and normalized to tissue-protein content. Dopamine content for each condition was taken as the average of the protein-normalized dopamine levels from the two coronal sections. Due to limits in animal numbers from each cohort and because rats could not be used for both histology and dopamine measurements, only a subset of rats were used for dopamine analysis while the majority of rats

were dedicated to histology and stereological measurements.

2.7. Histology

For histology, rats were deeply anesthetized with ketamine and xylazine and transcardially perfused with 0.9% saline for 3 min and 0.4% paraformaldehyde in PBS for 10 min at 30 mL/min using a peristaltic pump. Mice were anesthetized with 2,2,2-tribromoethanol (Alfa Aesar, 500 mg/kg body weight) and transcardially perfused with 0.9% saline for 1 min and 0.4% paraformaldehyde in PBS for 3 min at 8 mL/min. Brains were removed, post-fixed overnight in paraformaldehyde at 4 °C and cryoprotected in 30% sucrose in PBS for at least 72 h before flash-freezing in -45 °C isopentane on dry ice. Frozen brains were stored at -80 °C until sectioning on a cryostat (Leica CM1900). Free-floating sections (40 μ m thick) were collected in PBS prior to transfer and long-term storage in cryoprotectant solution (30% ethylene glycol, 30% glycerol in PBS).

2.8. Immunofluorescent staining of brain tissue

All steps were performed at room temperature. Sections were rinsed of cryoprotectant in PBS, blocked for 2 h in PBS with 0.2% Triton X-100 and 5% fetal bovine serum, and incubated overnight with primary antibodies (rabbit anti-tyrosine hydroxylase (TH), Pel-Freez, P40101-0, 1:1000; mouse anti-V5, Life Technologies, R960-25, 1:1000; rat anti-human- α -synuclein, Enzo Life Sciences, ALX-804-258-L001, 1:1000) in blocking buffer. Sections were rinsed with PBS and labeled for 2 h with fluorescent-tagged secondary antibodies (Life Technologies, 1:500). Rinsed sections were mounted onto slides and coverslipped with hardset Vectashield (Vector Labs, Burlingame, CA). The selectivity of the staining protocol was determined by omitting the primary antibodies in sections stained in parallel. Sections were imaged with a Keyence BZ 9000 Fluorescence Microscope. Immunofluorescent analyses were performed blinded with respect to genotype and drug with each animal given a numerical designation decoded after final counts were performed.

2.9. Immunoperoxidase-3,3'-diaminobenzidine staining

Immunohistochemical labeling of TH or phospho-serine129- α -synuclein (pS129-syn) was performed at room temperature on 40 μ m thick tissue sections. Sections were rinsed with Tris-buffered saline (TBS), and endogenous peroxidase activity was quenched for 5 min in TBS with 10% methanol and 3% H₂O₂. Rinsed sections were blocked for 2 h in TBS with 0.2% Triton X-100, 3% bovine serum albumin, 10% goat serum, and 1% glycine, and then incubated overnight with primary antibodies (rabbit anti-TH or rabbit anti-pS129-syn, Abcam, ab59264, 1:200) in blocking buffer. Sections were rinsed, incubated for 2 h with biotinylated goat anti-rabbit IgG (Vector Laboratories, BA-1000, 1:300) followed by streptavidin-conjugated horseradish peroxidase (Vectastain ABC kit, Vector Laboratories, PK-610, 1:300). Labeling was visualized with 0.003% hydrogen peroxide and 0.05% immunoperoxidase-3,3'-diaminobenzidine (DAB; Sigma) in 0.1 M Tris buffer, pH 8.0. Sections were mounted, dehydrated, and coverslipped with Eukitt Hard Set Mounting Media (Sigma). The selectivity of the staining protocol was determined by omitting the primary antibodies in sections stained in parallel. Images were acquired on a Keyence BZ 9000 Fluorescence Microscope in brightfield mode. The average intensity of TH in the striatum was quantified in ImageJ by drawing regions encompassing the dorsal striatum and subtracting the average background intensity of regions within the ipsilateral corpus callosum anterior commissure for each striatal hemisphere on each

slide. The average of three adjacent sections in the anterior striatum were used for each hemisphere of each animal. Histochemical analyses were performed blinded with respect to genotype and drug with each animal given a numerical designation decoded after final counts were performed.

2.10. Stereology

Total numbers of DAB-stained, TH-positive neurons in the SNC and ventral tegmental area (VTA) were estimated by stereological analysis using a computer-assisted image-analysis system consisting of an Olympus BX-51 microscope equipped with an XYZ computer-controlled motorized stage and an SIA-L9C Digital Camera (Scientific Instruments and Applications). Counts were made using the Optical Fractionator probe of Stereo Investigator software (MicroBrightField), as described previously (Berthet et al., 2014; Zhang et al., 2007). Each section was viewed at low magnification and the SNC and VTA were outlined separately. TH-positive neurons were counted with a 100 \times oil-immersion objective (NA 1.4) using a 75 \times 75 mm counting frame in a 150 \times 150 mm grid. For α -synuclein-injected rats, 7 sections were counted whereas in the older PINK1-KO rats, 8 sections were counted. Stereological analyses were performed blinded with respect to genotype and drug with each animal given a numerical designation decoded after final counts were performed.

2.11. Behavioral testing

All behavioral experiments were performed with the examiner blind to genotype. Open-field locomotor activity in both the horizontal and vertical fields was measured as previously described (Berthet et al., 2014; Shields et al., 2015). Performance traversing an elevated balance beam was performed as previously described (Carter et al., 1999) with minor changes. Prior to training or testing, mice were acclimated to the behavioral room for at least 60 min. On the first and second days of training, mice were trained with 3–5 trials to traverse the beam. On the third day, mice were tested on a thinner, more challenging beam and time to traverse, hind-foot slips, and complete falls from the beam were recorded. The averages of three trials were measured for each mouse.

2.12. Data analysis

Data are presented as mean \pm S.E. Statistical differences between conditions were analyzed using Prism 5.0 software by two-tailed *t*-test or two-way ANOVA with Newman-Keuls post-test, as specified in the figure legends. *p* values < 0.05 were considered significant.

3. Results

3.1. Long-term dosing of kinetin via chow

To boost PINK1 activity in the brain, we established a paradigm to chronically deliver the KTP-precursor kinetin using standard rodent chow (Purina 5053; Research Diets, Inc. NJ, USA). A previous study showed that this method effectively delivered kinetin into mouse brains, and that the maximal tolerated dose for mice was \sim 400 mg kinetin/kg body weight/day (Shetty et al., 2011). In our studies, we found that the maximal tolerated dose for control C57BL6 mice was 3.5 g kinetin/kg chow, corresponding to 400–600 mg kinetin/kg body weight/day, depending on the extent of age-dependent weight gain (Fig. 1A). In rats, supplementing the chow with bacon flavoring increased the tolerated dose to 5.25 g kinetin/kg chow, which achieved a maximal dose of \sim 300 mg

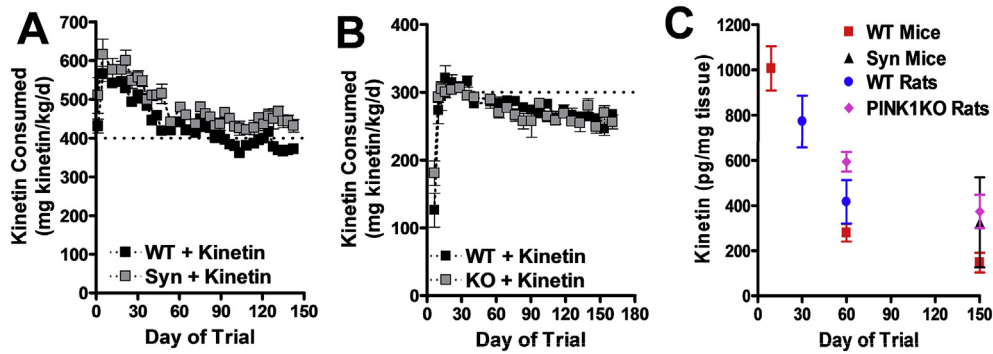


Fig. 1. Mice and rats tolerate long-term oral delivery of kinetin. (A) Consumption of kinetin in chow by WT or Syn mice during a 4.5-month trial (mean \pm SE, $n = 10$ WT and $n \geq 8$ Syn mice at all time points). (B) Consumption of kinetin by WT or PINK1 KO rats during a 5.5 month trial (mean \pm SE, $n = 4$ WT and $n \geq 9$ PINK1 KO rats at all time points). (C) Brain levels of kinetin measured by LC-MS in WT or transgenic mice or rats at the end of pilot or experimental trials of differing periods of chow consumption (mean \pm SE, $n \geq 3$).

kinetin/kg body weight/day for approximately 30 days. However, the maximal dose per weight declined slightly over time as the animals gained weight (Fig. 1B). Initially, the kinetin chow produced high levels of kinetin in the brain (~800–1000 pg/mg tissue); however, the levels decreased ~2–5-fold over more than 60 days with chronic feeding before plateauing (Fig. 1C), perhaps due to increased metabolic clearance in the periphery. No kinetin was detected in untreated brains.

3.2. Reintroduction of PINK1 using AAV vectors

Next, we tested if reintroducing WT PINK1 alone, but not G309D mutant PINK1, rescues neurodegeneration in PINK1 KO rats. We also evaluated if orally delivering kinetin can increase the extent of rescue, especially when reintroducing mutant G309D PINK1. To reintroduce WT and G309D mutant PINK1 into SNc DA neurons of PINK1 KO rats, we cloned PINK1 sequences with a C-terminal V5

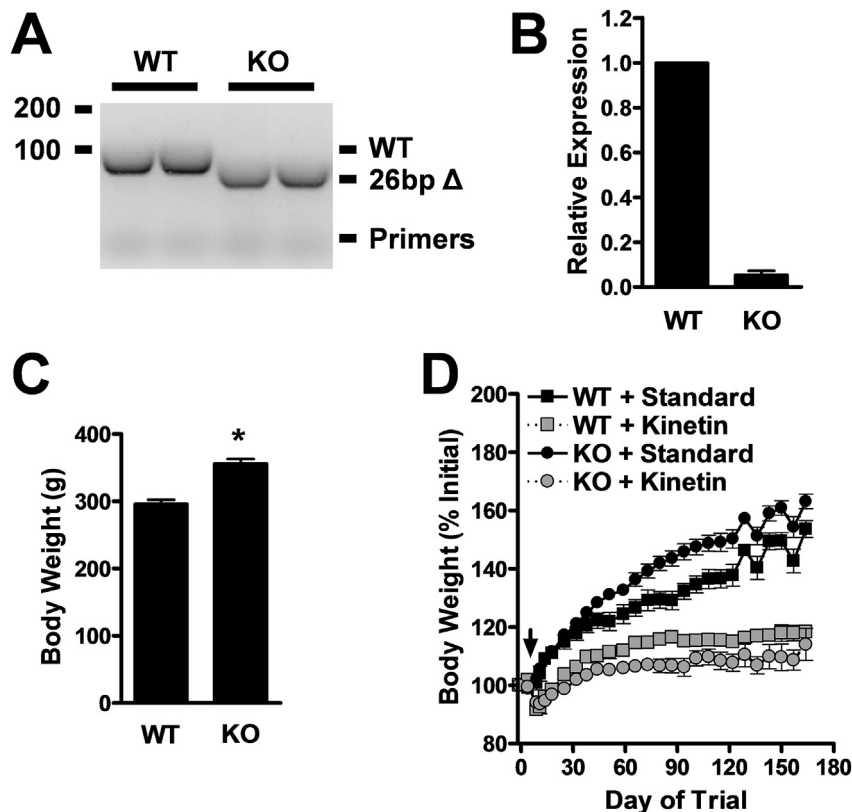


Fig. 2. PINK1 KO rats weigh more than WT rats, and both lose weight with prolonged kinetin delivery. (A) PCR genotyping products from WT and PINK1 KO rat-tail genomic DNA indicating expected 26 bp excision from the PINK1 gene in the PINK1 KO rats. (B) RT-qPCR genotyping of WT and PINK1 KO rats indicates near complete loss of PINK1 mRNA in brain tissue of PINK1 KO rats (mean \pm SE, $n = 3$). (C) Body weights of WT and PINK1 KO male rats at 10.5 weeks of age (mean \pm SE, $n = 13$ or 32 for WT or PINK1 KO, respectively). * $p < 0.0001$, Student's *t*-test. (D) Normalized body weights of WT and PINK1 KO male rats dosed for 5.5 months with either standard of kinetin chow (mean \pm SE, $n \geq 4$ at all time points). Note that groups are separated by genotype and chow, but that animals within groups received mixed bilateral injections of PBS or different AAV vectors during stereotaxic surgeries at Day of Trial 0. The black arrow indicates the switch to kinetin chow for appropriate cohorts.

epitope tag into AAV vectors under the control of the chicken β -actin promoter and prepared virus (serotype AAV2/6, UNC Vector Core) for stereotaxic brain injection. Tests in cultured primary hippocampal neurons showed low basal levels of PINK1-V5 expression basally (Supplementary Fig. 1A). Consistent with prior reports in which prolonged mitochondrial stress in neurons causes accumulation of PINK1 protein on the outer mitochondrial membrane (Narendra et al., 2010), PINK1-V5 levels increased substantially following depolarization with the uncoupler FCCP (Supplementary Fig. 1A). Following stereotaxic injection in the SNc of PINK1 WT and KO rats, both WT and G309D PINK1-V5 showed strong expression in DA neurons throughout the SN, as determined by TH immunofluorescence. In contrast, there was very little expression in the adjacent VTA, presumably because the virus remained localized to the SN (Supplementary Fig. 1B).

3.3. PINK1 KO rats do not show loss of DA neurons in the SNc

We confirmed the deletion of PINK1 from our PINK1 KO rats by genotyping (Fig. 2A) and the loss of PINK1 transcripts by RT-qPCR (Fig. 2B). PINK1 KO rats fed standard chow were significantly heavier than WT rats at 10 weeks of age (Fig. 2C), and they gained weight at an accelerated rate (Fig. 2D). These results contrast with

the decreased body weight in PINK1 KO mice (Gispert et al., 2009). Interestingly, prolonged delivery of high levels of kinetin reduced the weight of both KO and WT rats (Fig. 2D). This effect could be the result of metabolic changes that enhance clearance of kinetin (Fig. 1C).

Two previous reports showed that PINK1 KO rats have unique disturbances to their nigrostriatal pathway at 8–9 months of age. Although mitochondrial insults typically produce degeneration of DA axons before the cell body (Berthet et al., 2014; Pickrell et al., 2011; Pham et al., 2012; Betarbet et al., 2000), PINK1 KO rats lost ~ 50% of DA neurons in the SNc, without any loss of DA terminals in the striatum (Dave et al., 2014). To determine whether restoring PINK1 activity in DA neurons of PINK1 KO rats would prevent degeneration and restore DA content to WT levels, we reintroduced PINK1-WT and PINK1-G309D to the SNc at 2.5 months of age. Because PINK1-related PD is due to a near complete loss of PINK1 kinase activity, we expected PINK1-WT would significantly rescue degeneration, while PINK1-G309D would not. Injected rats were subsequently fed standard or kinetin chow for 5.5 months prior to quantitation of surviving DA neurons in the midbrain, the density of DA terminals, and total DA content in the dorsal striatum.

As previously reported by others (Dave et al., 2014), we observed

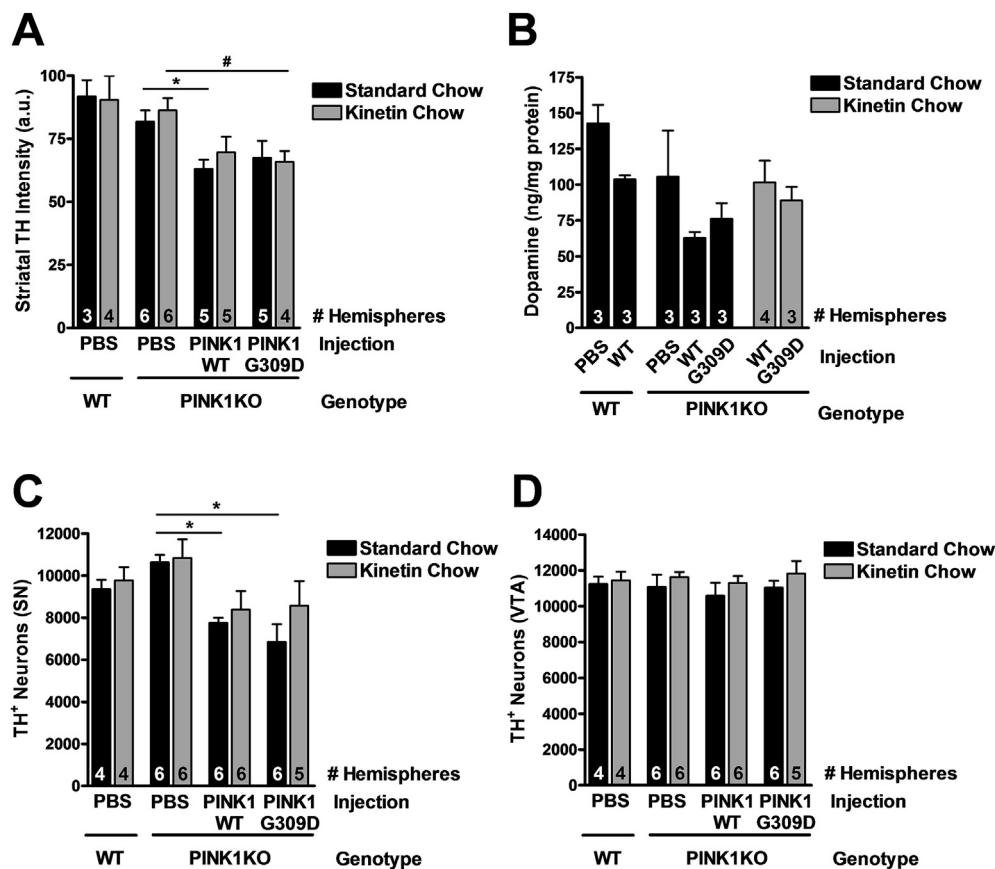


Fig. 3. The nigrostriatal pathway of PINK1 KO rats is intact. (A) TH-staining intensity in the dorsal striatum of WT or PINK1 KO rats injected with PBS or PINK1-V5 vectors and fed standard or kinetin chow for 5.5 months (mean \pm SE). Two-way ANOVA with Bonferroni post-test: $F(2,25) = 0.30$, $P = 0.74$ for interaction effect; $F(1,25) = 0.55$, $P = 0.46$ for chow effect; $F(2,25) = 8.09$ ($P = 0.002$) for virus effect. n indicated as “# Hemispheres” at the bottom of each bar. * $p < 0.05$ vs PINK1 KO with standard chow and PBS injection; # $p < 0.05$ vs PINK1 KO with kinetin chow and PBS injection. (B) DA content in the dorsolateral striatum of WT or PINK1 KO rats injected with PBS or PINK1-V5 vectors and fed standard or kinetin chow for 5.5 months (mean \pm SE, n indicated as “# Hemispheres” at the bottom of each bar). (C) Quantification of TH + neurons in the SNc of WT or PINK1 KO rats injected with PBS or PINK1-V5 vectors and fed standard or kinetin chow for 5.5 months (mean \pm SE). $F(2,29) = 0.49$, $P = 0.61$ for interaction effect; $F(1,29) = 1.85$, $P = 0.18$ for chow effect; $F(2,29) = 9.27$, $P = 0.0008$ for virus effect. n indicated as “# Hemispheres” at the bottom of each bar. * $p < 0.05$ vs PINK1 KO with standard chow and PBS injection; two-way ANOVA with Bonferroni post-test. (D) Quantification of TH + neurons in the VTA of WT or PINK1 KO rats injected with PBS or PINK1-V5 vectors and fed standard or kinetin chow for 5.5 months (mean \pm SE). $F(2,29) = 0.02$, $P = 0.98$ for interaction effect; $F(1,29) = 2.25$, $P = 0.14$ for chow effect; $F(2,29) = 0.45$, $P = 0.64$ for virus effect. n indicated as “# Hemispheres” at the bottom of each bar.

no significant difference in DA-terminal density in the striatum of PINK1 WT versus KO rats at 8 months of age (Fig. 3A). Prolonged kinetin did not affect the density of striatal DA terminals. However, re-expression of PINK1-WT and PINK1-G309D in PINK1 KO rats decreased the intensity of striatal TH staining by ~20% in both groups, suggesting either non-specific toxicity from overexpressing PINK1 (independent of kinase activity) and/or non-specific toxicity of the virus itself (Fig. 3A). In contrast to previous reports, however, we did not observe an increase in striatal DA levels in 8-month-old PINK1 KO rats (Fig. 3B). Instead, analysis of a small subset of rats ($n = 3$ per group) revealed a trend for decreased DA in the striatum of PINK1 KO rats ($p > 0.05$ for WT vs PINK1 KO hemispheres receiving PBS sham and WT PINK1 injections, respectively). There were also no significant effects of viral PINK1 expression or kinetin delivery, although there was a trend for decreased DA levels in hemispheres receiving either WT or mutant virus versus PBS sham ($p > 0.05$ for WT and PINK1 KO mice receiving WT virus, and for PINK1 KO mice receiving the G309D mutant PINK1). The lack of significance is likely due to the small number of samples assessed for DA levels and the high variability in the PINK1 KO PBS sham group (Fig. 3B). Unexpectedly, we observed no difference in the total number of DA neurons in the SN of PINK1 KO rats compared to WT rats at 8 months of age (Fig. 3C). Reintroducing PINK1-WT or

PINK1-G309D into the SN of PINK1 KO rats caused a small decrease in the number of DA neurons in both groups (Fig. 3C). Kinetin treatment caused a trend toward increased numbers of DA neurons, but these effects did not reach significance ($p > 0.05$). There were also no significant effects of PINK1 KO, viral injection, or chow on DA neuron counts in the VTA (Fig. 3D).

3.4. Kinetin in chow does not protect against α -synuclein-induced DA neurodegeneration

Excessive α -synuclein may underlie the pathophysiology of sporadic PD, which is characterized by α -synuclein-related pathology (Spillantini et al., 1998), in the context of WT PINK1 expression. However, without PINK1, the toxicity of mutant A53T α -synuclein is increased (Gispert et al., 2015), suggesting that boosting PINK1 activity may protect against excessive α -synuclein. Therefore, we tested whether activating endogenous PINK1 with kinetin alleviates DA toxicity due to α -synuclein overexpression via AAV in adult rats. Pilot studies indicated this model of α -synuclein toxicity resulted in ~66% loss of TH⁺ neurons in the SNc over 4 weeks. To allow time for kinetin conversion to KTP prior to peak α -synuclein expression, we fed rats kinetin chow 4 days before stereotaxic injection of PBS or AAV- α -synuclein into their SNc.

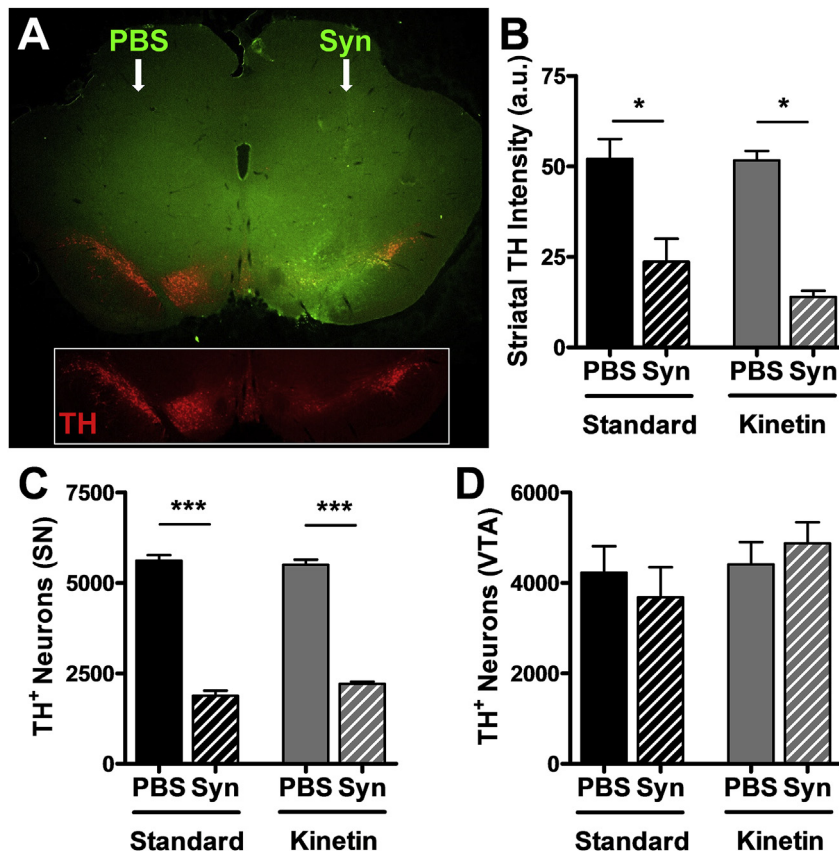


Fig. 4. Long-term kinetin does not protect against synuclein-induced neurotoxicity in rats. (A) Unilateral expression of α -synuclein (Syn, green) in the ventral midbrain following stereotaxic injection of PBS or AAV2-Syn in WT rats. Inset highlights the expression of TH (red) in DA neurons of the SN and VTA and the correlation between α -synuclein overexpression and loss of TH intensity. (B) TH-staining intensity in the dorsal striatum of WT rats injected with PBS or Syn vector and fed standard or kinetin chow for 1 month (mean \pm SE). Two-way ANOVA with Bonferroni post-test: $F(1,15) = 1.01$, $P = 0.33$ for interaction effect; $F(1,15) = 1.21$, $P = 0.29$ for chow effect; $F(1,15) = 52.04$, $p < 0.0001$ for virus effect. $n = 3$ –6 rats per group. * $p < 0.05$ vs PBS injection. (C) Quantification of TH + neurons in the SNc of WT rats injected with PBS or Syn vector and fed standard or kinetin chow for 1 month (mean \pm SE). Two-way ANOVA with Bonferroni post-test: $F(1,12) = 3.05$, $P = 0.11$ for interaction effect; $F(1,12) = 0.69$, $P = 0.42$ for chow effect; $F(1,12) = 737$, $p < 0.0001$ for virus effect. *** $p < 0.001$ vs PBS injection. (D) Quantification of TH + neurons in the VTA of WT rats injected with PBS or Syn vector and fed standard or kinetin chow for 1 month (mean \pm SE). Two-way ANOVA with Bonferroni post-test: $F(1,12) = 0.82$, $P = 0.38$ for interaction effect; $F(1,12) = 1.53$, $P = 0.24$ for chow effect; $F(1,12) = 0.00$, $p = 0.95$ for virus effect. $n = 4$ rats per group. (For interpretation of the references to colour in this figure legend, the reader is referred to the web version of this article.)

Immunofluorescence staining of α -synuclein and TH in the midbrain revealed strong expression of α -synuclein in the SN and VTA 4 weeks after injection and loss of TH immunoreactivity relative to the PBS-injected contralateral side (Fig. 4A). We quantified TH immunoreactivity in the striatum, which revealed significant loss of DA terminals due to α -synuclein overexpression, but no significant effect of kinetin consumption (Fig. 4B). There was a corresponding degeneration of DA neurons in the SNc caused by α -synuclein, but no significant effect of chronic kinetin consumption (Fig. 4C). No consistent effects of α -synuclein or kinetin were observed on DA neuron counts in the VTA (Fig. 4D), primarily because α -synuclein was more localized and strongly expressed in the SNc.

3.5. Chronic kinetin in chow does not prevent the behavioral or pathological effects of neuronal α -synuclein expression in mice

Next, we tested whether kinetin could reduce the severity of motor behavioral deficits and phosphorylated human α -synuclein (pS129-syn) pathology in transgenic mice overexpressing α -synuclein under the Thy1 neuron-specific promoter (Rockenstein et al., 2002). These mice have lower body weight, are hyperactive (prior to 6 months), and display impaired balance on a narrow-beam test (Chesselet et al., 2012). They also show age-dependent and region-specific accumulation of pS129-syn, a marker of Lewy Body

pathology in PD (Chesselet et al., 2012). Thy1-hSyn mice were switched to kinetin chow at weaning and remained on this chow throughout behavioral testing at 6 months of age. Kinetin did not affect the lowered body weight of these mice (Fig. 5A). As previously reported, Thy1-hSyn mice were hyperactive, and they displayed increased total movement and number of rearings in open-field assessments of behavior (Fig. 5B and C). However, chronic consumption of kinetin did not affect either activity measurement.

To test motor function, WT and Thy1-hSyn mice were monitored for their ability to traverse a narrow balance beam. Thy1-hSyn mice had an increased number of foot slips and falls from the balance beam, and they took longer to travel across the balance beam than WT mice (Fig. 5D–F). Oral kinetin significantly increased the number of foot slips and time to traverse the beam, and non-significantly increased the number of falls from the beam. The etiology of this worsening is unclear but may reflect specific PINK1-dependent or independent adverse effects on nervous system function. These changes in motor behavior were not associated with improved or worsened pS129-syn pathology in either the hippocampus (Fig. 6) or cortex (not shown).

4. Discussion

We urgently need therapeutics to prevent or slow neurodegeneration underlying PD. To this end, we tested whether oral

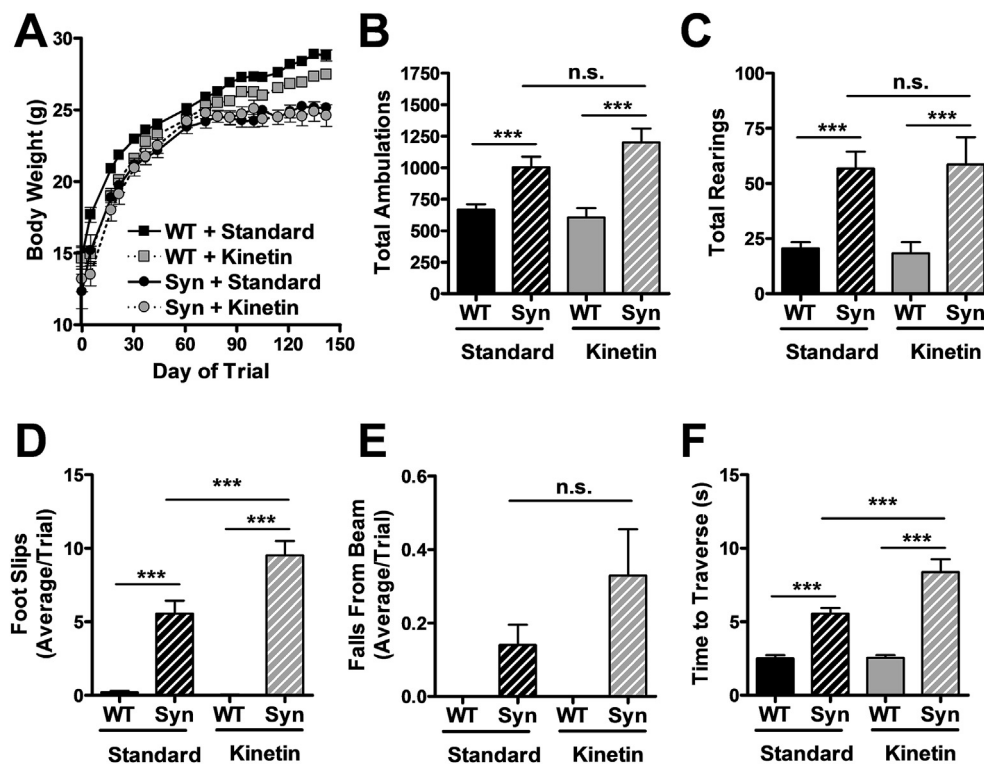


Fig. 5. Long-term kinetin does not improve behavior in synuclein-overexpressing mice. (A) Body weights of WT and Syn mice dosed for 4.5 months with either standard or kinetin chow (mean \pm SE, $n \geq 8$ at all time points). (B, C) Total movements and rearings of 6-month-old mice during the second half of a 15 min open-field behavioral test (mean \pm SE). (B) Two-way ANOVA with Bonferroni post-test: $F(1,36) = 2.61$, $P = 0.11$ for interaction effect; $F(1,36) = 0.68$, $P = 0.42$ for chow effect; $F(1,36) = 33.82$, $P < 0.0001$ for genotype effect. (C) Two-way ANOVA with Bonferroni post-test: $F(1,36) = 0.07$, $P = 0.79$ for interaction effect; $F(1,36) = 0.00$, $P = 0.99$ for chow effect; $F(1,36) = 26.74$, $P < 0.0001$ for genotype effect. $n = 10$ WT + standard chow, 10 WT + kinetin chow, 12 Syn + standard chow, 8 Syn + kinetin chow. *** $p < 0.001$ vs WT. n.s. indicates not significantly different at the $p < 0.05$ level. (D, E) Number of foot slips and falls of 6-month-old mice during the balance-beam motor performance test (mean \pm SE). (D) Two-way ANOVA with Bonferroni post-test: $F(1,33) = 11.90$, $P = 0.0016$ for interaction effect; $F(1,33) = 9.99$, $P = 0.0034$ for chow effect; $F(1,33) = 153.46$, $P < 0.0001$ for genotype effect. (E) Two-way ANOVA with Bonferroni post-test: $F(1,33) = 2.42$, $P = 0.1293$ for interaction effect; $F(1,33) = 2.42$, $P = 0.13$ for chow effect; $F(1,33) = 14.93$, $P = 0.0005$ for genotype effect. $n = 10$ WT + standard chow, 10 WT + kinetin chow, 9 Syn + standard chow, 8 Syn + kinetin chow. *** $p < 0.001$ vs WT. n.s. indicates not significantly different at the $p < 0.05$ level. (F) Time to traverse the balance beam by 6-month-old mice (mean \pm SE). Two-way ANOVA with Bonferroni post-test: $F(1,33) = 9.61$, $P = 0.0039$ for interaction effect; $F(1,33) = 10.17$, $P = 0.0031$ for chow effect; $F(1,33) = 96.76$, $P < 0.0001$ for genotype effect. $n = 10$ WT + standard chow, 10 WT + kinetin chow, 9 Syn + standard chow, 8 Syn + kinetin chow. *** $p < 0.001$ vs WT of same chow type or WT vs Syn with kinetin chow.

delivery of kinetin, a precursor of a PINK1 activator, was protective in rodent models of PD. Unfortunately, we found no evidence that kinetin protects in any of the model systems tested. For the α -synuclein models, our study clearly indicates that kinetin does not protect against α -synuclein overexpression when administered at the maximally tolerated oral dose. We wondered whether that dose of kinetin could produce a meaningful biologic activation of PINK1 activity, and whether restoring PINK1 function in adult animals can reverse neurodegeneration in PD models where genetic defects have been present since birth. Unfortunately, we were unable to answer these questions, because we did not observe the expected degeneration in PINK1 KO rats. This limitation highlights the need for more robust mammalian models of PINK1-induced DA neurodegeneration and biomarkers of PINK1 activity.

4.1. PINK1 KO rats do not consistently show SNc neurodegeneration

A major roadblock to the discovery and validation of PD therapeutics is the scarcity of transgenic rodent models that faithfully show age-dependent loss of DA neurons in the SNc. Initial reports (Dave et al., 2014; Villeneuve et al., 2016) suggested that PINK1 KO rats were a breakthrough model in this regard; however, we and others (Grant et al., 2015) failed to observe any degeneration of SNc DA neurons at the indicated 8-month time point. Notably, the degeneration may occur at later time points in our colonies, perhaps due to slower rates of degeneration caused by undetermined differences in the animals' environments. In our efforts to clarify these discrepancies, we observed no difference in DA neuron counts across multiple cohorts of animals. Although the number of animals in any particular group used for stereological counting was not large ($n = 4$ – 6 versus $n = 9$ in Dave et al. (2014)), there are several considerations that support our conclusion that no SNc degeneration occurs in our PINK1 KO rats up to 8 months of age. First, we observed a trend towards higher, not lower, DA neuron counts in the PINK1 KO versus WT rats, indicating that even much larger experimental groups would likely not show a significant decrease. Second, the counts were similar for the rat genotypes fed a standard or kinetin-supplemented chow. This lack of influence of the chow effectively doubles the number of comparisons between WT and PINK1 KO counts to a level similar to Dave et al. (Kitada

et al., 2007). Finally, we observed no loss of TH + terminals in the striatum. Dysregulation of DA was reported in the original description of the PINK1 KO rats (Dave et al., 2014), and loss of DA axons consistently precedes loss of cell bodies in the SNc in other pharmacologic and genetic mitochondrial-based models of DA neuron degeneration (Berthet et al., 2014; Pickrell et al., 2011; Pham et al., 2012; Betarbet et al., 2000) and in PD (Cheng et al., 2010; Chu et al., 2012). Collectively, our observations raise concerns about using the PINK1 KO rat model to study neurodegeneration in the SNc and highlight a need to further characterize this model beyond 8 months of age.

4.2. Oral kinetin insufficiently protects against α -synuclein-related toxicity

Strategies to prevent α -synuclein-dependent pathology are a major focus in the search for therapeutics against sporadic PD. We observed a lack of protection with oral kinetin in rodent models of α -synuclein neurodegeneration. These findings suggest that either kinetin-dependent activation of endogenous PINK1 inadequately combats α -synuclein-driven pathology, or that oral delivery of therapeutics does not reach adequate thresholds of kinetin delivery or PINK1 activation. To maximize the brain levels of kinetin we used the highest tolerated doses, but still observed a decline in these levels with chronic dosing. We chose the oral route of administration to best model the likely delivery in human patients, and because this method has been successfully used in mice (Shetty et al., 2011). Future studies using intraventricular mini-pumps or twice-daily IP injections may be needed to evaluate the efficacy of higher doses and test the efficacy of alternative ATP analogs that activate PINK1. Once optimized, additional trials with lower levels of virally expressed α -synuclein may be warranted.

4.3. Kinetin does have biological effects

We found that oral kinetin affected the behavior of Thy1-hSyn mice in ways similar to changes observed with another mitochondrial modulator, the cholesterol oxime TRO40303 (Richter et al., 2014). TRO40303 binds to the mitochondrial translocator protein (TSPO) and is broadly neuroprotective. Interestingly, both

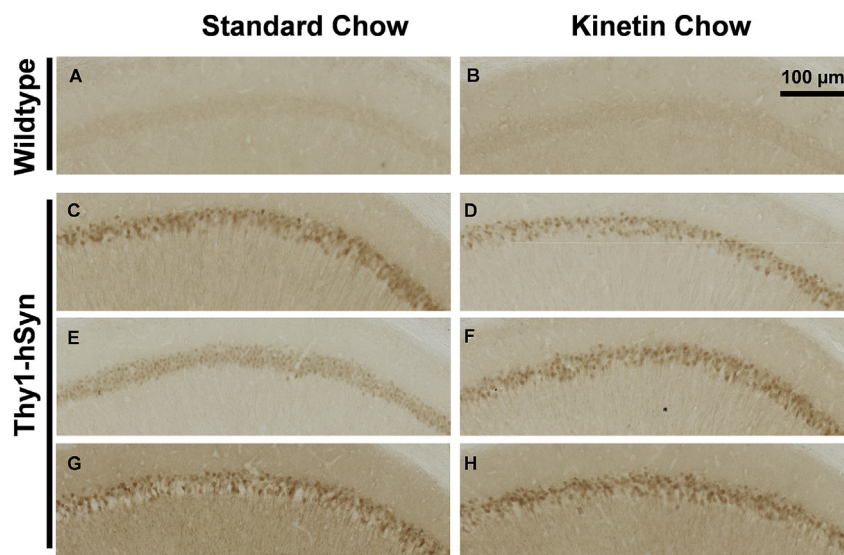


Fig. 6. Long-term kinetin does not reduce pS129-Synuclein pathology in Thy1-hSyn mice. pS129-Synuclein staining in the CA1 region of the hippocampus of 6-month-old WT (A–B) or Syn (C–H) mice dosed for 4.5 months with standard or kinetin chow. Scale bar = 100 μ m.

kinetin and TRO40303 increased the number of foot slips on the balance-beam motor behavior test with Thy1-hSyn mice. This similar effect may indicate successful engagement between kinetin (KTP) and PINK1 at neuronal mitochondria. However, PINK1 also may not have been effectively engaged during these studies. Future work will need to incorporate biomarkers of PINK1 engagement, and perhaps levels of phosphorylated ubiquitin, phospho complex I, or other PINK1 phospho-targets. Currently, using antibody-based immunostaining or blotting, we were unable to identify reliable biomarkers that are sensitive, selective, or dependent on PINK1 expression in our models. To better establish a protective role for PINK1 activation and to identify valuable biomarkers for PINK1 activation, we will need more robust mammalian models of PINK1 deficiency. If PINK1 loss alone is not sufficiently toxic in these systems, then PINK1 loss may need to be studied in the setting of a second mitochondrial insult that increases the need for PINK1.

Ultimately, given that kinetin has biological effects in neuronal systems (Hertz et al., 2013), as well as an established safety profile in humans for short-term use (Gold-von Simson et al., 2009), we believe that preliminary testing of kinetin in patients with PINK1 kinase activity may still be warranted, even if kinetin cannot be preclinically validated in rodent models of PINK1 deficiency. Although our data suggest that kinetin may not be protective in models of sporadic PD, it may still be effective in patients with inherited mutations in PINK1. Unfortunately, due to the limitations of existing models of PINK1 deficiency, preclinical testing of PINK1 activators in rodents may not be informative in predicting clinical efficacy. As such, with the existing safety record of kinetin, there is a reasonable argument for proceeding directly to early stage testing in at-risk families. Despite the limited number of PINK1-deficient patients, success in even this small subset of PD patients would still be a major clinical advance and provide badly needed proof-of-principle evidence that beginning disease-modifying therapy in adulthood can indeed treat a genetic form of PD.

Funding

This work was supported by Mitokinin LLC, the Joan and David Traitel Family Trust, and NIH (1R01NS091902 to K.N. and RR018928 to the Gladstone Institutes). The experiments were designed by KN and AO with guidance from members of Mitokinin (NH, DR and KS). Mitokinin was not involved in the collection, analysis, writing or submission of the report.

Acknowledgements

The authors would like to thank the following people who provided technical support or advice to this project: Amandine Berthet and Jiasheng Zhang for assistance and training with stereology; R. Jude Samulski (University of North Carolina) and the University of North Carolina Vector Core for providing the pTR-CBA-eGFP vector and advice on AAV cloning; Meaghan Morris, Lennart Mucke and Eliezer Masliah for providing the Thy1-hSyn mice; T. Michael Gill, Iris Lo and Ryan Craft (Gladstone Behavioral Core) for assistance with behavioral testing; The Familial Dysautonomia Foundation (New York, NY) and Susan Slaughaupt (Harvard Medical School) for advice on oral delivery of kinetin to rodents; Erica Nguyen for administrative assistance and Crystal Herron for assistance editing the manuscript.

Appendix A. Supplementary data

Supplementary data related to this article can be found at <http://dx.doi.org/10.1016/j.neuint.2017.04.006>.

References

- Berthet, A., Margolis, E.B., Zhang, J., Hsieh, I., Zhang, J., Hnasko, T.S., et al., 2014. Loss of mitochondrial fission depletes axonal mitochondria in midbrain dopamine neurons. *J. Neurosci.* 34 (43), 14304–14317.
- Betarbet, R., Sherer, T.B., MacKenzie, G., Garcia-Osuna, M., Panov, A.V., Greenamyre, J.T., 2000. Chronic systemic pesticide exposure reproduces features of Parkinson's disease. *Nat. Neurosci.* 3 (12), 1301–1306.
- Carter, R.J., Lione, L.A., Humby, T., Mangiarini, L., Mahal, A., Bates, G.P., et al., 1999. Characterization of progressive motor deficits in mice transgenic for the human Huntington's disease mutation. *J. Neurosci.* 19 (8), 3248–3257.
- Cheng, H.C., Ulane, C.M., Burke, R.E., 2010. Clinical progression in Parkinson disease and the neurobiology of axons. *Ann. Neurol.* 67 (6), 715–725.
- Chesselet, M.F., Richter, F., Zhu, C., Magen, I., Watson, M.B., Subramaniam, S.R., 2012. A progressive mouse model of Parkinson's disease: the Thy1-aSyn ("Line 61") mice. *Neurotherapeutics* 9 (2), 297–314.
- Chinta, S.J., Mallajosyula, J.K., Rane, A., Andersen, J.K., 2010. Mitochondrial alpha-synuclein accumulation impairs complex I function in dopaminergic neurons and results in increased mitophagy in vivo. *Neurosci. Lett.* 486 (3), 235–239.
- Chu, Y., Morfini, G.A., Langhamer, L.B., He, Y., Brady, S.T., Kordower, J.H., 2012. Alterations in axonal transport motor proteins in sporadic and experimental Parkinson's disease. *Brain* 135 (Pt 7), 2058–2073.
- Clark, I.E., Dodson, M.W., Jiang, C., Cao, J.H., Huh, J.R., Seol, J.H., et al., 2006. *Drosophila pink1* is required for mitochondrial function and interacts genetically with parkin. *Nature* 441 (7097), 1162–1166.
- Dagda, R.K., Pien, I., Wang, R., Zhu, J., Wang, K.Z., Callio, J., et al., 2014. Beyond the mitochondrion: cytosolic PINK1 remodels dendrites through protein kinase A. *J. Neurochem.* 128 (6), 864–877.
- Dauer, W., Kholodilov, N., Vila, M., Trillat, A.C., Goodchild, R., Larsen, K.E., et al., 2002. Resistance of alpha-synuclein null mice to the parkinsonian neurotoxin MPTP. *Proc. Natl. Acad. Sci. U. S. A.* 99 (22), 14524–14529.
- Dave, K.D., De Silva, S., Sheth, N.P., Rambo, S., Beck, M.J., Quang, C., et al., 2014. Phenotypic characterization of recessive gene knockout rat models of Parkinson's disease. *Neurobiol. Dis.* 70, 190–203.
- Devi, L., Raghavendran, V., Prabhu, B.M., Avadhani, N.G., Anandatheerthavarada, H.K., 2008. Mitochondrial import and accumulation of alpha-synuclein impair complex I in human dopaminergic neuronal cultures and Parkinson disease brain. *J. Biol. Chem.* 283 (14), 9089–9100.
- Gispert, S., Ricciardi, F., Kurz, A., Azizov, M., Hoepken, H.H., Becker, D., et al., 2009. Parkinson phenotype in aged PINK1-deficient mice is accompanied by progressive mitochondrial dysfunction in absence of neurodegeneration. *PLoS One* 4 (6), e5777.
- Gispert, S., Brehm, N., Weil, J., Seidel, K., Rub, U., Kern, B., et al., 2015. Potentiation of neurotoxicity in double-mutant mice with Pink1 ablation and A53T-SNCA overexpression. *Hum. Mol. Genet.* 24 (4), 1061–1076.
- Gold-von Simson, G., Goldberg, J.D., Rolnitzky, L.M., Mull, J., Leyne, M., Voustianiouk, A., et al., 2009. Kinetin in familial dysautonomia carriers: implications for a new therapeutic strategy targeting mRNA splicing. *Pediatr. Res.* 65 (3), 341–346.
- Grant, L.M., Kelm-Nelson, C.A., Hilby, B.L., Blue, K.V., Paul Rajamanickam, E.S., Pultorak, J.D., et al., 2015. Evidence for early and progressive ultrasonic vocalization and oromotor deficits in a PINK1 gene knockout rat model of Parkinson's disease. *J. Neurosci. Res.* 93 (11), 1713–1727.
- Haddad, D., Nakamura, K., 2015. Understanding the susceptibility of dopamine neurons to mitochondrial stressors in Parkinson's disease. *FEBS Lett.* 589 (24 Pt A), 3702–3713.
- Haque, M.E., Thomas, K.J., D'Souza, C., Callaghan, S., Kitada, T., Slack, R.S., et al., 2008. Cytoplasmic Pink1 activity protects neurons from dopaminergic neurotoxin MPTP. *Proc. Natl. Acad. Sci. U. S. A.* 105 (5), 1716–1721.
- Haque, M.E., Mount, M.P., Safarpour, F., Abdel-Messih, E., Callaghan, S., Mazerolle, C., et al., 2012. Inactivation of Pink1 gene in vivo sensitizes dopamine-producing neurons to 1-methyl-4-phenyl-1,2,3,6-tetrahydropyridine (MPTP) and can be rescued by autosomal recessive Parkinson disease genes, Parkin or DJ-1. *J. Biol. Chem.* 287 (27), 23162–23170.
- Hertz, N.T., Berthet, A., Sos, M.L., Thorn, K.S., Burlingame, A.L., Nakamura, K., et al., 2013. A neo-substrate that amplifies catalytic activity of parkinson's-disease-related kinase PINK1. *Cell* 154 (4), 737–747.
- Hnasko, T.S., Chuhma, N., Zhang, H., Goh, G.Y., Sulzer, D., Palmiter, R.D., et al., 2010. Vesicular glutamate transport promotes dopamine storage and glutamate corelease in vivo. *Neuron* 65 (5), 643–656.
- Ibanez, P., Bonnet, A.M., Debarges, B., Lohmann, E., Tison, F., Pollak, P., et al., 2004. Causal relation between alpha-synuclein gene duplication and familial Parkinson's disease. *Lancet* 364 (9440), 1169–1171.
- Itoh, K., Nakamura, K., Iijima, M., Sesaki, H., 2013. Mitochondrial dynamics in neurodegeneration. *Trends Cell Biol.* 23 (2), 64–71.
- Kamp, F., Exner, N., Lutz, A.K., Wender, N., Hegermann, J., Brunner, B., et al., 2010. Inhibition of mitochondrial fusion by alpha-synuclein is rescued by PINK1, Parkin and DJ-1. *EMBO J.* 29 (20), 3571–3589.
- Kane, L.A., Lazarou, M., Fogel, A.L., Li, Y., Yamano, K., Sarraf, S.A., et al., 2014. PINK1 phosphorylates ubiquitin to activate Parkin E3 ubiquitin ligase activity. *J. Cell Biol.* 205 (2), 143–153.
- Kitada, T., Pisani, A., Porter, D.R., Yamaguchi, H., Tschertner, A., Martella, G., et al., 2007. Impaired dopamine release and synaptic plasticity in the striatum of PINK1-deficient mice. *Proc. Natl. Acad. Sci. U. S. A.* 104 (27), 11441–11446.

- Koyano, F., Okatsu, K., Kosako, H., Tamura, Y., Go, E., Kimura, M., et al., 2014. Ubiquitin is phosphorylated by PINK1 to activate parkin. *Nature* 510 (7503), 162–166.
- Kruger, R., Kuhn, W., Muller, T., Woitalla, D., Graeber, M., Kosel, S., et al., 1998. Ala30Pro mutation in the gene encoding alpha-synuclein in Parkinson's disease. *Nat. Genet.* 18 (2), 106–108.
- Li, W.W., Yang, R., Guo, J.C., Ren, H.M., Zha, X.L., Cheng, J.S., et al., 2007. Localization of alpha-synuclein to mitochondria within midbrain of mice. *Neuroreport* 18 (15), 1543–1546.
- Lin, W., Wadlington, N.L., Chen, L., Zhuang, X., Brorson, J.R., Kang, U.J., 2014. Loss of PINK1 attenuates HIF-1alpha induction by preventing 4E-BP1-dependent switch in protein translation under hypoxia. *J. Neurosci.* 34 (8), 3079–3089.
- Liu, G., Zhang, C., Yin, J., Li, X., Cheng, F., Li, Y., et al., 2009. alpha-Synuclein is differentially expressed in mitochondria from different rat brain regions and dose-dependently down-regulates complex I activity. *Neurosci. Lett.* 454 (3), 187–192.
- Loeb, V., Yakunin, E., Saada, A., Sharon, R., 2010. The transgenic over expression of alpha-synuclein and not its related pathology, associates with complex I inhibition. *J. Biol. Chem.* 285 (10), 7334–7343.
- Morais, V.A., Verstreken, P., Roethig, A., Smet, J., Snellinx, A., Vanbrabant, M., et al., 2009. Parkinson's disease mutations in PINK1 result in decreased Complex I activity and deficient synaptic function. *EMBO Mol. Med.* 1 (2), 99–111.
- Morais, V.A., Haddad, D., Craessaerts, K., De Bock, P.J., Swerts, J., Vilain, S., et al., 2014. PINK1 loss-of-function mutations affect mitochondrial complex I activity via Ndufa10 ubiquinone uncoupling. *Science* 344 (6180), 203–207.
- Nakamura, K., Nemani, V.M., Azarbal, F., Skibinski, G., Levy, J.M., Egami, K., et al., 2011. Direct membrane association drives mitochondrial fission by the Parkinson disease-associated protein alpha-synuclein. *J. Biol. Chem.* 286 (23), 20710–20726.
- Narendra, D., Tanaka, A., Suen, D.F., Youle, R.J., 2008. Parkin is recruited selectively to impaired mitochondria and promotes their autophagy. *J. Cell Biol.* 183 (5), 795–803.
- Narendra, D.P., Jin, S.M., Tanaka, A., Suen, D.F., Gautier, C.A., Shen, J., et al., 2010. PINK1 is selectively stabilized on impaired mitochondria to activate Parkin. *PLoS Biol.* 8 (1), e1000298.
- Orr, A.L., Vargas, L., Turk, C.N., Baaten, J.E., Matzen, J.T., Dardov, V.J., et al., 2015. Suppressors of superoxide production from mitochondrial complex III. *Nat. Chem. Biol.* 11 (11), 834–836.
- Park, J., Lee, S.B., Lee, S., Kim, Y., Song, S., Kim, S., et al., 2006. Mitochondrial dysfunction in *Drosophila* PINK1 mutants is complemented by parkin. *Nature* 441 (7097), 1157–1161.
- Pathak, D., Shields, L.Y., Mendelsohn, B.A., Haddad, D., Lin, W., Gerencser, A.A., et al., 2015. The role of mitochondrially derived ATP in synaptic vesicle recycling. *J. Biol. Chem.* 290 (37), 22325–22336.
- Pham, A.H., Meng, S., Chu, Q.N., Chan, D.C., 2012. Loss of Mfn2 results in progressive, retrograde degeneration of dopaminergic neurons in the nigrostriatal circuit. *Hum. Mol. Genet.* 21 (22), 4817–4826.
- Pickrell, A.M., Pinto, M., Hida, A., Moraes, C.T., 2011. Striatal dysfunctions associated with mitochondrial DNA damage in dopaminergic neurons in a mouse model of Parkinson's disease. *J. Neurosci.* 31 (48), 17649–17658.
- Polymeropoulos, M.H., Lavedan, C., Leroy, E., Ide, S.E., Dehejia, A., Dutra, A., et al., 1997. Mutation in the alpha-synuclein gene identified in families with Parkinson's disease. *Science* 276 (5321), 2045–2047.
- Poole, A.C., Thomas, R.E., Andrews, L.A., McBride, H.M., Whitworth, A.J., Pallanck, L.J., 2008. The PINK1/Parkin pathway regulates mitochondrial morphology. *Proc. Natl. Acad. Sci. U. S. A.* 105 (5), 1638–1643.
- Puschmann, A., Fiesel, F.C., Caulfield, T.R., Hudec, R., Ando, M., Truban, D., et al., 2017. Heterozygous PINK1 p.G411S increases risk of Parkinson's disease via a dominant-negative mechanism. *Brain* 140 (Pt 1), 98–117.
- Ricciardi, L., Petrucci, S., Guidubaldi, A., Ialongo, T., Serra, L., Ferraris, A., et al., 2014. Phenotypic variability of PINK1 expression: 12 Years' clinical follow-up of two Italian families. *Mov. Disord.* 29 (12), 1561–1566.
- Richter, F., Gao, F., Medvedeva, V., Lee, P., Bove, N., Fleming, S.M., et al., 2014. Chronic administration of cholesterol oximes in mice increases transcription of cyto-protective genes and improves transcriptome alterations induced by alpha-synuclein overexpression in nigrostriatal dopaminergic neurons. *Neurobiol. Dis.* 69, 263–275.
- Rockenstein, E., Mallory, M., Hashimoto, M., Song, D., Shults, C.W., Lang, I., et al., 2002. Differential neuropathological alterations in transgenic mice expressing alpha-synuclein from the platelet-derived growth factor and Thy-1 promoters. *J. Neurosci. Res.* 68 (5), 568–578.
- Shetty, R.S., Gallagher, C.S., Chen, Y.T., Hims, M.M., Mull, J., Leyne, M., et al., 2011. Specific correction of a splice defect in brain by nutritional supplementation. *Hum. Mol. Genet.* 20 (21), 4093–4101.
- Shields, L.Y., Kim, H., Zhu, L., Haddad, D., Berthet, A., Pathak, D., et al., 2015. Dynamin-related protein 1 is required for normal mitochondrial bioenergetic and synaptic function in CA1 hippocampal neurons. *Cell Death Dis.* 6, e1725.
- Singleton, A.B., Farrer, M., Johnson, J., Singleton, A., Hague, S., Kachergus, J., et al., 2003. alpha-Synuclein locus triplication causes Parkinson's disease. *Science* 302 (5646), 841.
- Song, S., Jang, S., Park, J., Bang, S., Choi, S., Kwon, K.Y., et al., 2013. Characterization of PINK1 (PTEN-induced putative kinase 1) mutations associated with Parkinson disease in mammalian cells and *drosophila*. *J. Biol. Chem.* 288 (8), 5660–5672.
- Spillantini, M.G., Crowther, R.A., Jakes, R., Hasegawa, M., Goedert, M., 1998. alpha-Synuclein in filamentous inclusions of Lewy bodies from Parkinson's disease and dementia with lewy bodies. *Proc. Natl. Acad. Sci. U. S. A.* 95 (11), 6469–6473.
- Valente, E.M., Abou-Sleiman, P.M., Caputo, V., Muqit, M.M., Harvey, K., Gispert, S., et al., 2004. Hereditary early-onset Parkinson's disease caused by mutations in PINK1. *Science* 304 (5674), 1158–1160.
- Villeneuve, L.M., Purnell, P.R., Boska, M.D., Fox, H.S., 2016. Early expression of Parkinson's disease-related mitochondrial abnormalities in PINK1 knockout rats. *Mol. Neurobiol.* 53 (1), 171–186.
- Wang, X., Winter, D., Ashrafi, G., Schlehe, J., Wong, Y.L., Selkoe, D., et al., 2011. PINK1 and Parkin target Miro for phosphorylation and degradation to arrest mitochondrial motility. *Cell* 147 (4), 893–906.
- Zarranz, J.J., Alegre, J., Gomez-Esteban, J.C., Lezcano, E., Ros, R., Ampuero, I., et al., 2004. The new mutation, E46K, of alpha-synuclein causes Parkinson and Lewy body dementia. *Ann. Neurol.* 55 (2), 164–173.
- Zhang, J., Pho, V., Bonasera, S.J., Holtzman, J., Tang, A.T., Hellmuth, J., et al., 2007. Essential function of HIPK2 in TGFbeta-dependent survival of midbrain dopamine neurons. *Nat. Neurosci.* 10 (1), 77–86.